Materials Physics and Mechanics 47 (2021) 872-884
Research article

Received: August 9, 2021
Accepted: November 19, 2021

EFFECT OF THE DISTANCE BETWEEN CATHODE AND SUBSTRATE ON STRUCTURAL AND OPTICAL PROPERTIES OF ZINC OXIDE THIN FILMS DEPOSITED BY RF SPUTTERING TECHNIQUE

Mohibul Khan, Sk. Faruque Ahmed✉

Nanoscience Laboratory, Department of Physics, Aliah University, IIA/27, Newtown, Kolkata-700160, India

✉ fahmed.phys@aliah.ac.in

Abstract. Zinc oxide (ZnO) thin films have been fabricated over glass substrates via Radio Frequency (RF) sputtering technique with varying distances between cathode and substrate. The aim of the fabrication of thin films was to study the structural, morphological, compositional, and optical properties by varying the distance between cathode and substrate. X-Ray Diffractometer (XRD) has been used to discuss the structural property of deposited thin films. The XRD patterns of fabricated ZnO thin films indicate wurtzite hexagonal crystal phase at miller indices (002) by a high intense peak at the Bragg's angle 34.4^{o}. Crystallite size of fabricated ZnO thin films decreases from 32 nm to 17 nm with increasing the distance between cathode and substrate from 65 nm to 125 nm respectively, which have been calculated using XRD (002) peak. The information about morphological characteristics of the surface of ZnO thin films has been discussed by using Atomic Force Microscope. Some information about the bonding of fabricated ZnO thin films has been studied by Fourier Transform Infrared Spectroscopy. UV-VIS spectrophotometer has been used to investigate the optical property and Urbach parameter of the deposited ZnO thin films. Optical energy, which is also known as bandgap energy, increases from 3.16 eV to 3.25 eV with increasing the distance between cathode and substrate from 65 nm to 125 nm respectively. Urbach energy i.e., defect density decreases from 195 meV to 182 meV with the increasing the distance between cathode and substrate from 65 nm to 125 nm respectively. The change in optical transmittance, optical band gap energy, and Urbach energy has been discussed in terms of nanostructure ZnO thin films.

Keywords: ZnO thin films, RF sputtering technique, XRD, FT-IR, Optical bandgap energy, Urbach energy

Acknowledgements. *One of the authors (M. Khan) wishes to acknowledge the University Grants Commission, New Delhi, India for the financial support under Maulana Azad National Fellowship (MANF) scheme during the execution of the work.*

Citation: Khan M., Ahmed S.F. Effect of the distance between cathode and substrate on structural and optical properties of zinc oxide thin films deposited by RF sputtering technique // Materials Physics and Mechanics. 2021, V. 47. N. 6. P. 872-884. DOI: 10.18149/MPM.4762021_7.

http://dx.doi.org/10.18149/MPM.4762021_7

1. Introduction

In current decades semiconducting transparent materials are highly acceptable for their usable behaviour in optoelectronic device technology. A large number of researchers have focused on ZnO material because ZnO is the most attractive transparent conducting oxide (TCO) material [1]. Semiconducting materials are widely applicable in science and technical fields for their changeable optical bandgap and very short-range wavelength. Environmentally safe ZnO is one of the greatest significant n-type II-VI chalcogenide semiconducting materials, which have a direct large bandgap (3.37 eV) and wide exciton binding energy (60 meV) [2-4]. The hexagonal wurtzite crystal structure of ZnO thin films occupies the piezoelectric oscillator property [2,5,6]. Such kind of II-VI semiconductor thin films has been widely explained as a result of their extensive applications in optoelectronic devices [7-9]. ZnO thin films demonstrate a few extra aspects and show a large number of naturalistic benefits like good transparency, chemical stability, non-toxic, well luminescence property, and prominent electron mobility at room temperature [2,3]. As a result of these exceptional features ZnO thin films are broadly used as photovoltaic cells, light-emitting diodes, solar cells, UV protectors, antibacterial coatings, chemical sensors, spintronics, cancer treatment, smart windows, gas sensing devices, electroluminescent devices, photocatalysis, flat panel displays, high mobility transistor, computer screen, transparent conducting oxides, varistors, Schottky diodes, drug delivery devices, surface acoustic devices, high electron mobility, transparent electrodes, smartphone display, thin-film transistor and laser diodes [2-5,7-15].

Physical and chemical methods have been used to fabricated ZnO thin films such as chemical vapour deposition, dip coating, successive ionic layer absorption and reaction (SILAR), chemical bath deposition, pulsed laser deposition, low-temperature aqueous solution route, metal-organic chemical vapor deposition, electron beam evaporation, thermal evaporation, chemical co-precipitation method, molecular beam epitaxy, sol-gel preparation, hydrothermal method, RF sputtering, spray pyrolysis, DC sputtering, screen printing, photochemical deposition, co-reactive magnetron sputtering technique, simultaneous DC and RF magnetron sputtering techniques and electrochemical deposition [2,3,14,16-19]. RF sputtering technique is an extremely acceptable process for the fabrication of nano range thin films. Such a method has lots of demerits like the excellent quality of thin films over low-temperature growth, conventional methods, direct control of thin films thickness, wide surface area coverage, and well morphological surface.

In this scientific research work, ZnO thin films have been fabricated on glass substrates by RF sputtering technique where the target of ZnO is used in RF cathode. ZnO thin films have been fabricated on glass substrates by changing the gap between cathode and substrate from 65 mm to 125 mm respectively and also investigate their structural and optical properties. Fabricated ZnO thin films are characterized and analyzed by using X-Ray Diffractometer (XRD), Atomic Force Microscope (AFM), Fourier Transform Infrared Spectroscopy (FT-IR), and UV-VIS Spectrophotometer. Optical transparency, as well as optical band gap energy of the fabricated ZnO thin films, has been determined from the transmittance spectra by using UV-VIS spectroscopy. The change in optical band gap energy and Urbach band tail of ZnO thin films have been described in detail.

2. Experimental details

Materials and deposition techniques. ZnO thin films were fabricated on a glass substrate via RF sputtering technique with a variety of distance between cathode and substrate from 65 mm to 125 mm respectively. All the ZnO thin films were deposited at room temperature (30^{o}C) for 30 minutes. ZnO target of purity 99.999%, diameter 2.125 inches, and thickness 2 mm was used as source material (cathode), which has been purchased from Sigma-Aldrich Company. Commercial glass of length 75 mm, width 25 mm, and thickness 1.45 mm has been

used as a substrate for the fabrication of ZnO thin films using RF sputtering technique. Acetone and distilled water have been used to clean all glass substrates by using ultrasonic vibration at 40^{o}C temperatures. Then all glass substrates were rinsed thoroughly with distilled water several times. The air gun was used to dry water-soaked glass substrate.

RF power supply was used to sputter the ZnO target. The objectionable impurities of the ZnO target were removed by pre-sputtering of Argon (Ar) gas for 10 minutes. At first, the deposition chamber was vacuumed by Rotary pump and then also Turbo pump respectively. Base pressure of the chamber was maintained at 3.0×10^{-4} Pa using Turbo pump. Deposition pressure was maintained by Ar and Oxygen gas of 14 sccm and 4 sccm respectively. Ar and oxygen gas were maintained into the vacuum chamber by using a mass flow controller (MFC). Ar gas was used here for its good sputtering behaviour. Oxygen gas has been used in the deposition chamber for controlling the oxygen capacity growth environment that is highly significant for the decrement of the intrinsic donor defects. The working pressure was maintained at 2.5 Pa by using Ar and oxygen gas. The surface morphology, uniform film thickness, and regular array of grains in the ZnO thin films have been controlled by a rotating substrate's rotator, which has fixed 3 rotations per minute. Distance between ZnO target i.e., cathode and substrate were varied from65 mm to 125 mm respectively. RF power supply has been used to fabricate ZnO thin films, which is set at 90 watts. Details of deposition conditions are given below Table 1.

Table 1. Deposition conditions maintained for the formation of nanocrystal ZnO thin films

Deposition parameters	**Deposition values**
Base pressure	3.0×10^{-4} Pa
Working pressure	2.5 Pa
Target	ZnO
Argon gas	14 sccm
Oxygen gas	4 sccm
Deposition temperature	30^{o}C
Substrate rotate	3 rpm
RF power	90 watt
Deposition time	30 minutes
Cathode to substrate distance	65 mm, 85 mm, 105 mm, and 125 mm

Characterizations. The structural, morphological, chemical composition, and optical properties of ZnO thin films were investigated. The crystalline structure of ZnO thin films was investigated by using X-ray Diffractometer (Bruker, D-8 Advance). The morphological characteristics of the surface of thin films were studied by using AFM (Bruker, MultiMode-8) ambient-based multimode AFM. AFM measurements of fabricated thin films were done in contact mode. A silicon probe was used for the scanning purpose, which had a radius of curvature 10 nm, height 15 microns with a standard chip size of 1.6×1.6×0.4 mm. Cross-sectional scanning electron microscope has been used to measure the thickness of all fabricated ZnO thin films, which was found uniform. The appropriate information about the chemical bonding of atoms and molecules in the fabricated thin films was studied by using FT-IR spectroscopy (IR Affinity-1S, Shimadzu, Japan). UV-Vis spectrophotometer (V-770, Jasco, Japan) has been used to study the optical transmittance spectra of fabricated ZnO thin films within the UV-VIS region.

3. Results and discussions

XRD analysis. The structural crystallinity of fabricated ZnO thin films has been characterized by XRD. Figure 1 represents the XRD patterns of ZnO thin films on the glass substrates, which was found in Bragg's angle between 20^o to 70^o using the source voltage 40 KV and source current 40 mA by using the Cu-Kα radiation of wavelength $\lambda = 1.5406$Å. The scan rate of the deposited thin films was two degrees per minute. The ZnO thin films have two kinds of crystal structures like hexagonal wurtzite or cubic zinc blende, which is available naturally [3-5,9,20]. The XRD patterns of the deposited thin films indicate wurtzite hexagonal phase at miller indices (002) by a high intense peak at the Bragg's angle 34.4^o, which was matched with JCPDS card no 36-1451 [11,14]. The intensities of the deposited thin films were decreased slowly with increasing distance between cathode and substrate from 65 mm to 125 mm respectively.

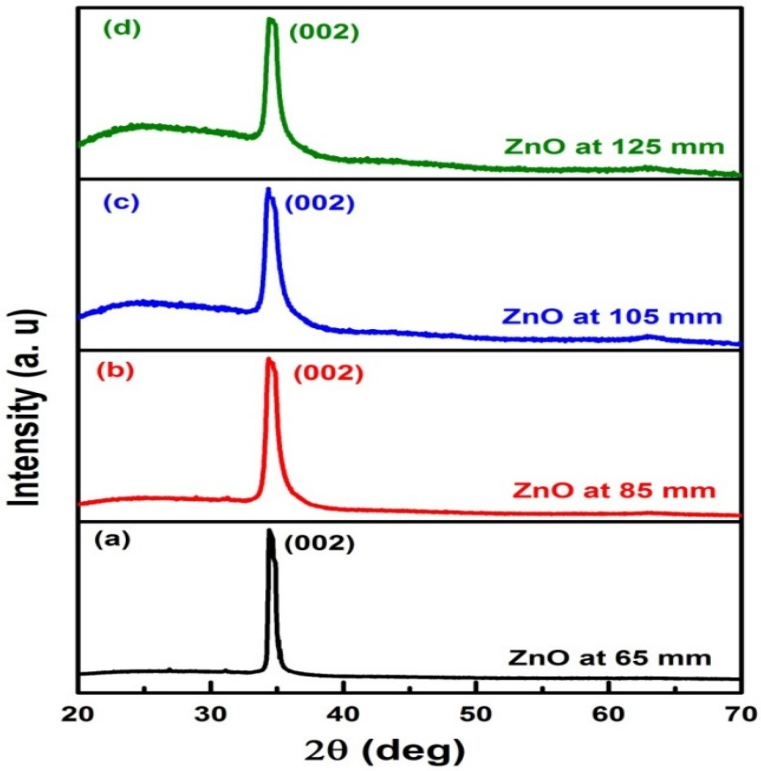

Fig. 1. XRD patterns of ZnO thin films fabricated over glass substrates; (a) 65 mm, (b) 85 mm, (c) 105 mm and (d) 125 mm

Equation 1 is known as the Debye-Scherrer formula, which was used to measure the crystallite sizes *(D)* of the deposited thin films [3,14,21]

$$D^{-1} = (\beta cos\theta)/K\lambda, \quad (1)$$

where $K = 0.94$ is known as Scherer constant, $\lambda = 1.5406$Å is known as the wavelength of X-ray, β is known as the full width of half maximum (FWHM) and θ is known as Bragg's angle. It was observed that the crystallite size of thin films was reduced from 32 nm to 17 nm with the increasing distance between cathode and substrate from 65 mm to 125 mm respectively. As crystallite size is inversely related to FWHM, so crystallite sizes are reduced from 32 nm to 17 nm with increasing FWHM from 0.2716^o to 0.5108^o respectively [14]. Strain (ε) of thin films was calculated using equation 2 [14,21].

$$\frac{1}{\varepsilon} = \frac{4}{\beta cos\theta}, \quad (2)$$

Strain of fabricated ZnO thin films varies from 11.3×10^{-4} to 21.3×10^{-4} with increasing distance between cathode and substrate from 65 mm to 125 mm respectively. Strain of deposited thin films is inversely changed with the crystallite size. The Variation of FWHM, Strain, and Crystallite size with respect to the cathode to substrate distance of fabricated ZnO thin films has been shown in Fig. 2. Equation 3 is known as Bragg's equation, which was used to measure the interplanar spacing (d) of the synthesized thin films. [4,21]

$$\frac{1}{d} = (2sin\theta)/n\lambda, \quad (3)$$

where n is known as the order of diffraction. Equation 4 is used to calculate the lattice constant c of the fabricated ZnO thin films [4].

$$d^{-2} = [\left(\frac{4}{3a^2}\right)(h^2 + hk + k^2)] + l^2c^2, \quad (4)$$

where lattice constants are a and c. The lattice constant c of fabricated ZnO thin films increases very slightly from 5.204 Å to 5.222 Å.

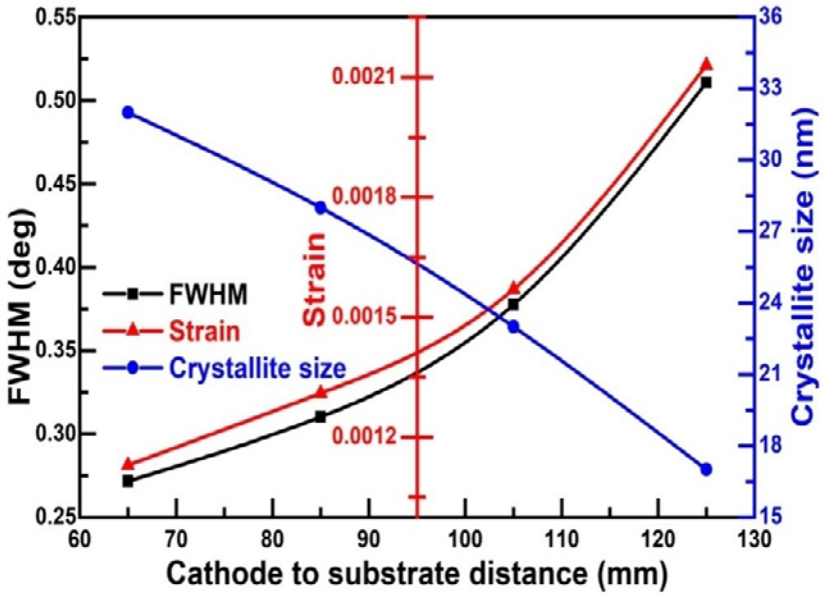

Fig. 2. Variation of FWHM, strain, and crystallite size with respect to the cathode to substrate distance

It was noticed that with the increasing strain, the crystallite size was decreased and lattice constants were increased respectively [14]. The values of glancing angles (2θ), FWHM (β), crystallite sizes (D), strain (ε), interplanar spacing (d), and lattice constant (c) are shown in Table 2.

Table 2. XRD data of ZnO thin films at the different distances between cathode and substrate

Cathode to Substrate distance (mm)	Bragg's Angle in degree (2θ)	FWHM (β) in degree	Crystallite sizes $D = K\lambda/\beta cos\theta$ in nm	Interplanar spacing $d = \lambda/2sin\theta$ in (Å)	Strain $\varepsilon = (\frac{\beta cos\theta}{4}) \times 10^{-4}$	Lattice constant c (Å)
65	34.43	0.2716	32	2.602	11.3	5.204
85	34.42	0.3102	28	2.603	13.1	5.206
105	34.36	0.3776	23	2.607	15.7	5.214
125	34.32	0.5108	17	2.611	21.3	5.222

AFM study. AFM was used to study the morphological effect on the surface of the deposited thin films. The accurate image of deposited thin films was captured by a highly resolute scanning probe AFM micrograph. Naturally, the deposited thin films were found identical and ordinary. Figures 3(a) and (b) represent the Two-dimensional (2-D) AFM images of ZnO thin films. AFM images of the deposited thin films show that morphological behaviour changes with increasing the distance between cathode and substrate from 65 mm to 125 mm respectively. Reflecting and scattering properties of the transmittance light depend on the morphological rough surfaces of the deposited thin films. Grain sizes of the deposited thin films decrease with a decrease in morphological roughness of the surfaces. Where morphological roughness of the surface decreases with increasing the distance between cathode to the substrate from 65 mm to 125 mm respectively. Histogram of the AFM images (Fig. 3 c-d) shows that the grain sizes of the thin films change from 38 nm to 20 nm with increasing the distance between cathode to the substrate from 65 mm to 125 mm respectively. The grain size as measured in the AFM image of deposited ZnO thin films is much higher than that calculated from the XRD data of the same films. The grain size measured in the AFM image can be greater than the crystallite size estimated from XRD. The reason for getting bigger crystallite size as observed on the AFM surface morphology of the films is due to the agglomeration of smaller crystals, while the XRD provides information about average crystallite size that coherently scatters X-rays [22,23].

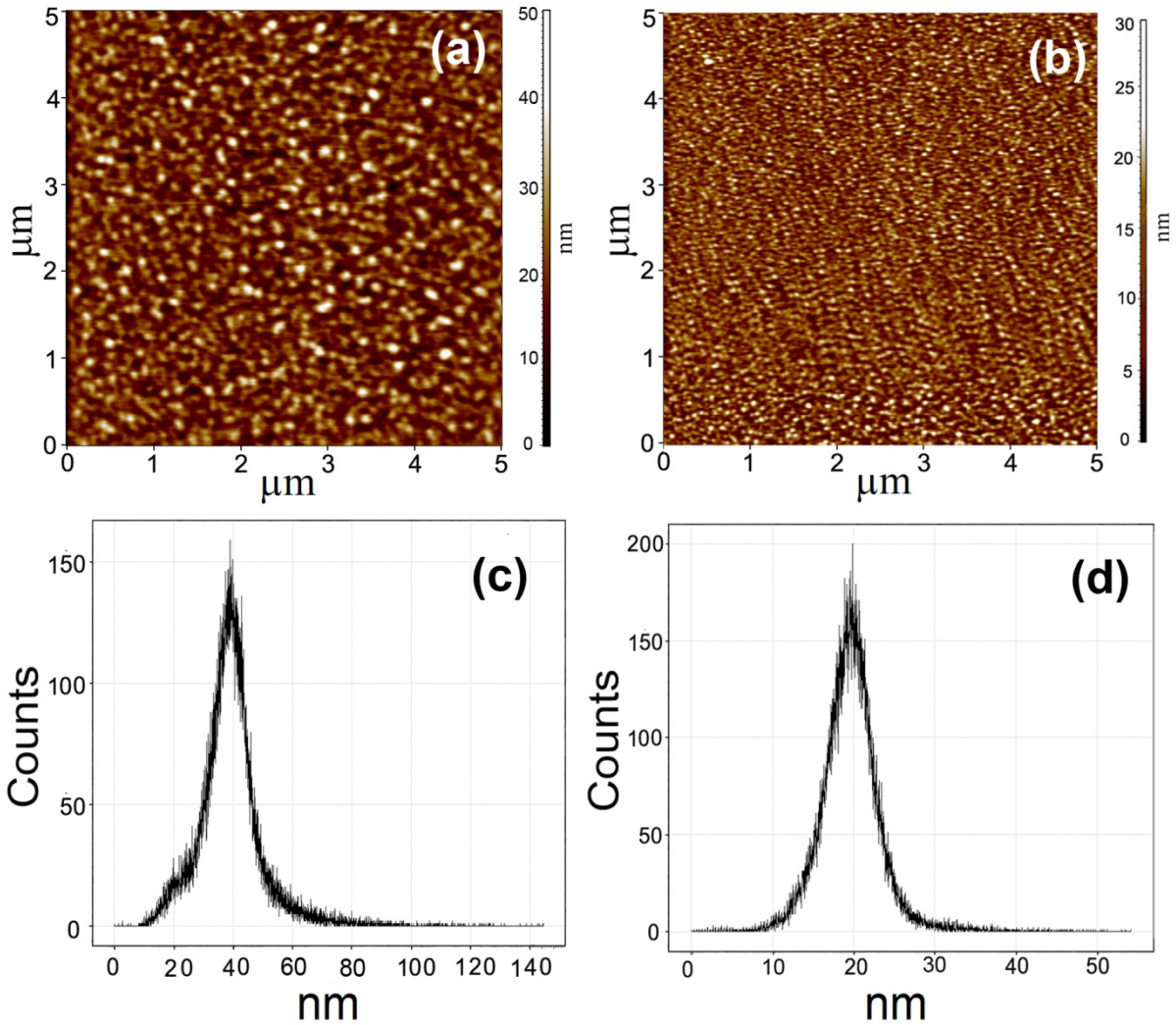

Fig. 3. 2-D AFM images of ZnO thin films deposited with different cathode to substrate distance; (a) 65 mm, (b) 125 mm, (c) and (d) the corresponding histogram

FT-IR study. Figure 4 represents the FT-IR image of ZnO thin films fabricated over a glass substrate. Chemical information about atoms and molecules of the thin films were investigated by FT-IR spectroscopy in the range of wave number 400 cm^{-1} to 4000 cm^{-1}. The absorption spectra of the FT-IR were used to select the absorption peak of the ZnO thin films where the reference was plane glass substrate. Structural and molecular information of the fabricated ZnO thin films has been analyzed by the FT-IR spectrum. Wave numbers within 400 cm^{-1} to 4000 cm^{-1} of the FT-IR spectra are separated into two parts. The first part within 400 cm^{-1} to 1600 cm^{-1} is familiar as a fingerprint region and the other part within 1600 cm^{-1} to 4000 cm^{-1} is familiar as a functional group region. In the fingerprint region of the FT-IR spectra only stretching and bending vibration happen whereas only stretching vibration happens in the functional group region. The stretching and bending vibration is responsible for forming the FT-IR absorption spectra of deposited ZnO thin films. The peak intensity of several atoms or molecular bonds depends on various materials. Peak intensity has changed with changing distance between cathode and substrate from 65 mm to 125 mm. The absorption peak of the Zn-O bond has been found near 586 cm^{-1} which confirmed that deposited thin films are ZnO thin films [24]. One strong absorption peak was found near 820 cm^{-1} which was attributed due to the stretching vibration of C-C bond [25]. Absorption peaks of FT-IR spectra near 1520 cm^{-1} and 1710 cm^{-1} were attributed due to symmetric stretching of C=O band [26-28]. Two other CO absorption peaks were found on the oxide surface of the thin films between wave number 2010 cm^{-1} to 2180 cm^{-1} [29]. The peak situated near 2348 cm^{-1} was attributed as a result of CO_2 molecules in the thin films, which were formed at the time of formation of thin films or CO_2 molecules in the atmosphere [30,31]. The wide absorption peak made within 3725 cm^{-1} to 3865 cm^{-1} was ascribed as a result of O-H or C-H bond stretching vibrations of hydroxyl groups present in the thin films or as a result of the atmosphere at the time of FT-IR analysis [2,26].

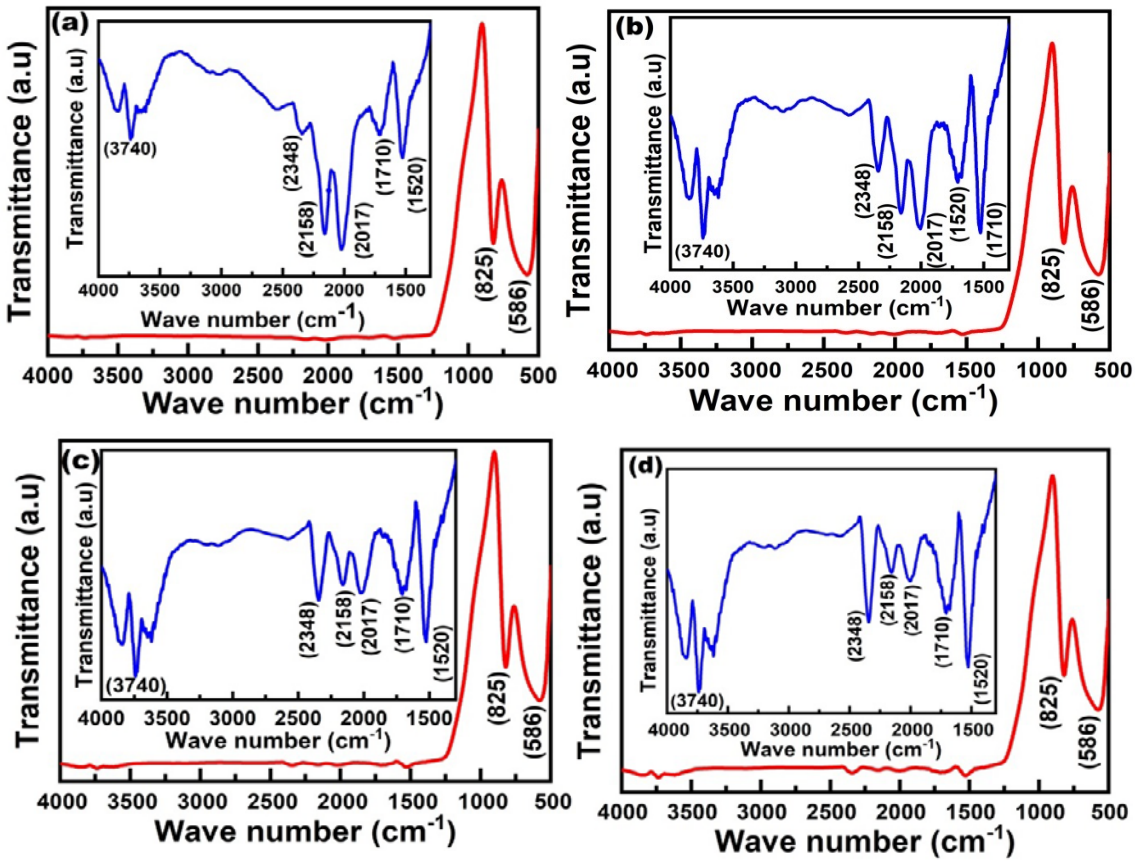

Fig. 4. FT-IR spectra of ZnO thin films; (a) 65 mm, (b) 85 mm, (c) 105 mm and (d) 125 mm

Optical study. UV-Vis spectrophotometer has been used to study the optical transmittance spectra of ZnO thin films fabricated over glass substrate at room temperature in the UV-visible region of wavelength 300 nm to 800 nm. The mean transmittance value was found between 87%-95% for ZnO thin films, which have been fabricated on a glass substrate with changing the distance between cathode and substrate from 65 mm to 125 mm respectively. Figure 5(a) exhibits that in the visible region deposited thin films have high transmittance, which clearly informs that the fabricated thin films are very good characteristics of optical properties as a result of low scattering or absorption losses. Figure 5(a) also indicates that transmittances spectra of fabricated thin films have been shifted from near UV region to visible region and also moderately decreased with the increasing the distance between cathode and substrate.

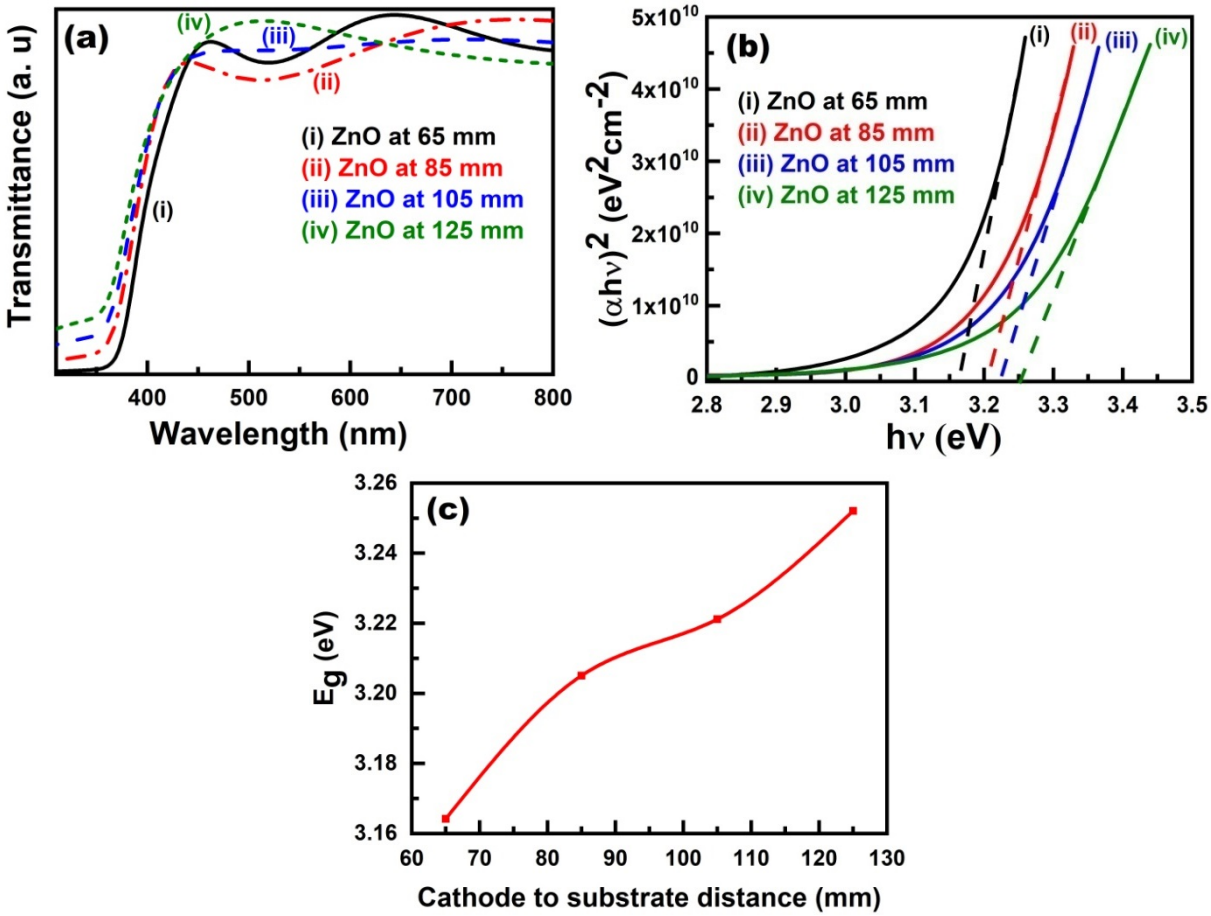

Fig.5. (a) Transmission spectra of ZnO thin films with the variation of distance between cathode and substrate (b) Tauc plot of $(\alpha h\nu)^2$ versus hν for the variation of distance between cathode and substrate, (c) variation of bandgap energy (E_g) with respect to the different cathode and substrate distance

Optical transmittance of the deposited ZnO thin films was decreased may be as a result of decreasing the thickness of the thin films [32]. Cross-sectional Scanning Electron Microscope has been used to measure the thickness of the fabricated ZnO thin films, which indicates that the thickness of the thin films decreased from 380 nm to 250 nm with increasing the distance between cathode and substrate from 65 mm to 125 mm respectively. Absorption coefficient (α) of fabricated ZnO thin films has been measured by using Beer-Lambert law using equation (5), which has been taken from the band theory of solids [4,21]

$$I_t = I_0\, e^{-\alpha t}, \tag{5}$$

where I_0 is indicated as the intensity of incident light and I_t is indicated as the intensity of transmitted light, t is known as the thickness of the fabricated ZnO thin films. From equation (5), the optical transmittance relation is simplified as $T = \frac{I_t}{I_0}$, which is known as simplifying relation of Beer-Lambert equation. Using the Tauc expression, the energy of optical band gap (E_g) of ZnO thin films has been calculated by fitting absorption co-efficient data [21,33,34]

$$(\alpha h\nu)^{1/m} = B(h\nu - E_g), \quad (6)$$

where B, α, m, and $h\nu$ are indicated as a constant, absorption coefficient, nature of electronic transition, and energy of the incident photon (h, ν are indicated as Planck's constant and incident light frequency). The optical bandgap energy of the deposited thin films depends on different fabrication materials. Where the value of m depends on transition quality. There are four types as 1/2, 2, 3/2, and 3 for the transitions of direct allowed, indirect allowed, direct forbidden, and indirect forbidden respectively [4,33,35]. Here the value of m is used as 1/2, because ZnO is a directly allowed transition material [4]. Figure 5(b) represents the graph of $(\alpha h\nu)^2$ versus $h\nu$ of ZnO thin films. The optical bandgap energy of fabricated ZnO thin films has been determined from this graph. The appearance of a single slope in $(\alpha h\nu)^2$ versus $h\nu$ graph indicates that fabricated thin films have directly allowed transition.

The optical bandgap energy of fabricated ZnO thin films has been calculated from the extrapolation of the straight-line portion of the $(\alpha h\nu)^2 = 0$ on the x-axis. It has been found that the energy of the optical bandgap of the fabricated nanocrystal ZnO thin films is inversely related to the crystallite size [36]. The crystallite size of ZnO thin films decreased from 32 nm to 17 nm where the bandgap increased from 3.16 eV to 3.25 eV respectively. Figure 5(c) indicates that the energy of the optical band gap of ZnO thin films increases from 3.16 eV to 3.25 eV as a result of increasing the distance between cathode and substrate from 65 mm to 125 mm respectively.

Urbach energy. Urbach band tail, which is known as Urbach energy, is used to determine the disorder of the fabricated ZnO thin films. Urbach energy (E_u) is defined as the band tail width connected within the forbidden gap of localised states in the crystal structure of fabricated ZnO thin films as shown in Fig. 6(a). Urbach Energy (E_u) can be expressed from Fig. 6(a)

$$E_u = \Delta \mathrm{E}_g - \Delta \mathrm{E}_{g/}, \quad (7)$$

where ΔE_g indicates the gap between the valence to the conduction band and $\Delta E_{g/}$ indicates the gap between the tails of the valence to the conduction band. Urbach energy, which provides information about the disorder or defect density, is calculated from the exponential function below the slope of the absorption edge [37-39]. Disorderness of phonon states of fabricated nano range ZnO thin films has been shown by Urbach energy. The band tail width, which is entitled Urbach energy, has been found under the absorption edge of the compound. The absorption edge of the optical bandgap has been formed as a result of interaction within exciting-phonon or maybe as a result of interaction within electron-phonon. Urbach energy of ZnO thin films as it may be calculated from the steepness parameter of absorption edge as a result of optoelectronic transfer within excited states and near localized states. The transition's band bending is a result of subtraction of the optical bandgap. The disorderness of the fabricated ZnO thin films will be high in the phonon states if the Urbach energy is higher. The Urbach energy of ZnO thin films has been found by fitting an exponential function to the slope of the absorption edge gives disorderness or defect density. The Urbach energy of fabricated ZnO thin films is expressed by the equation [21,37,41,42]

$$ln\alpha = ln\alpha_0 - h\nu/E_u, \quad (8)$$

where α, α_0 and $h\nu$ are indicated as absorption coefficient, constant, and incident photon energy respectively. Band tail of Urbach of semiconductor chalcogenide materials depends on

some possible defects like structural disorder, carrier-impurity interaction and carrier-phonon interaction, etc [39]. The Urbach energy (E_u) is associated with the width of the band tail, which is formulated as a result of the existence of localized states below the optical bandgap [5,40]. Urbach energy of ZnO thin films has been calculated from the plot of $ln\alpha$ versus $h\nu$, which is shown in Fig. 6(b) where the slope is linear. The Urbach band tail in the crystalline structure of phonon states of deposited thin films straight provides some helpful information around the thermal disorderness or the occupancy level [39]. Usually, the energy of the optical band gap of fabricated thin films is inversely related to the Urbach energy [39]. The current work reveals that Urbach energy of the fabricated ZnO thin films decreases whereas optical bandgap energy increases. Urbach energy of fabricated ZnO thin films was decreased from 195 meV to 182 meV with increasing the distance between cathode to the substrate from 65 mm to 125 mm respectively, which has shown in Fig. 6(c). Urbach energy of fabricated ZnO thin films was decreased from 195 meV to 182 meV as the thickness of thin films decreased from 380 nm to 250 nm. Decreasing Urbach energy i.e., the defect density of ZnO thin films was observed for Co-doped ZnO thin films, which has been affecting the optical characteristics of semiconductor chalcogenide materials [32].

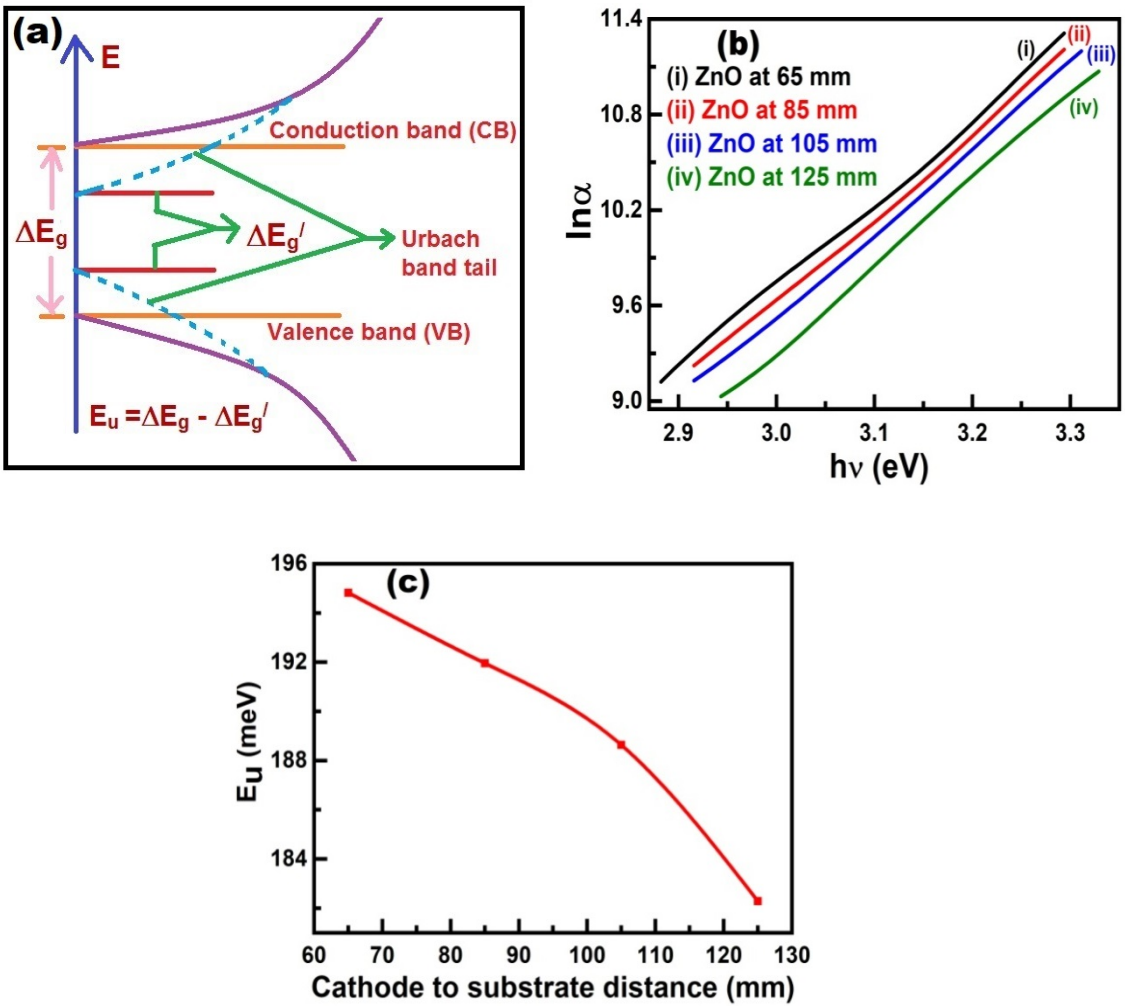

Fig. 6. (a) Schematic diagram of Urbach band tail, (b) a plot of lnα vs. hν of ZnO thin films, (c) Variation of Urbach energy (E_u) of ZnO thin films with respect to the distance between cathode to substrate

4. Conclusions

In this scientific research work, RF sputtering technique has been used to fabricate ZnO thin films on the glass substrates. XRD result indicates that the fabricated ZnO thin films have a wurtzite crystal structure with preferential orientation (002). Crystallite size of ZnO thin films was calculated from XRD pattern, which reduced from 32 nm to 17 nm with increasing distance between cathode to substrate from 65 mm to 125 mm respectively. The absorption peak of the Zn-O bond was found near 586 cm^{-1} in the FT-IR spectrum, which confirmed the fabricated films are ZnO thin films. The AFM analysis showed that the grain size was decreased with increasing distance between cathode to substrate. As the distance between cathode to substrate increased from 65 mm to 125 mm, the value of film thickness decreased from 380 nm to 250 nm and the value of optical bandgap energy increased from 3.16 eV to 3.25 eV. Urbach energy of the fabricated thin films was decreased from 195 meV to 182 meV with an increased distance between cathode to substrate from 65 mm to 125 mm respectively at room temperature $30^{o}C$. The nanocrystalline ZnO thin films were demonstrated with controlling its transparency and optical bandgap by changing the distance between cathode to substrate could have potential use in optical devices.

References

[1] Hafdallah A, Djefaflia F, Saidane N. Structural and Optical Properties of ZnO Thin Films Deposited by Pyrolysis Spray Method: Effect of Substrate Temperature. *Optics.* 2018;7(2): 68-73.

[2] Sajjad M, Ullah I, Khan M, Khan J, Khan MY, Qureshi MT. Structural and optical properties of pure and copper doped zinc oxide nanoparticles. *Results Phys*. 2018;9: 1301-1309.

[3] Imran M, Ahmed R, Afzal N, Rafique M. Copper ion implantation effects in ZnO film deposited on flexible polymer by DC magnetron sputtering. *Vacuum*. 2019;165: 72-80.

[4] Yusof AS, Hassan Z, Zainal N. Fabrication and characterization of copper doped zinc oxide by using Co-sputtering technique. *Mater. Res. Bull*. 2018;97: 314-318.

[5] Maiti UN, Ghosh PK, Ahmed SF, Mitra MK, Chattopadhyay KK. Structural, optical and photoelectron spectroscopic studies of nano/micro ZnO: Cd rods synthesized via sol-gel route. *J. Sol-Gel Sci. Technol*. 2007;41: 87-92.

[6] Mukherjee N, Ahmed SF, Chattopadhyay KK, Mondal A. Role of solute and solvent on the deposition of ZnO thin films. *Electrochimica Acta*. 2009;54(16): 4015-4024.

[7] Caglar Y, Caglar M, Ilican S, Aksoy S, Yakuphanoglu F. Effect of channel thickness on the field effect mobility of ZnO-TFT fabricated by sol gel process. *J. Alloys Compd*. 2015;621: 189-193.

[8] Al-Hardan NH, Abdullah MJ, Ahmad H, Aziz AA, Low LY. Investigation on UV photodetector behaviour of RF-sputtered ZnO by impedance spectroscopy. *Solid State Electron*. 2011;55(1): 59-63.

[9] Khosravi P, Karimzadeh F, Salimijazi HR, Abdi Y. Structural, optical and electrical properties of co-sputtered p-type ZnO:Cu thin-films. *Ceram. Int*. 2019;45(6): 7472-7479.

[10] Kim H, Pique A, Horwitz JS, Murata H, Kafafi ZH, Gilmore CM, Chrisey DB. Effect of aluminum doping on zinc oxide thin films grown by pulsed laser deposition for organic light-emitting devices. *Thin Solid Films*. 2000;377: 798-802.

[11] Zargar RA, Khan SUD, Khan MS, Arora M, Hafiz AK. Synthesis and Characterization of Screen Printed Zn0.97Cu0.03O Thick Film for Semiconductor Device Applications. *Phys. Res. Int*. 2014;2014: 464809.

[12] Isherwood PJM. Copper Zinc Oxide: Investigation into a p-type mixed metal oxide system. *Vacuum*. 2017;139: 173-177.

[13] Pandey B, Ghosh S, Srivastava P, Kabiraj D, Shripati T, Lalla NP. Synthesis of nano dimensional ZnO and Ni-doped ZnO thin films by atom beam sputtering and study of their physical properties. *Physica E*. 2009;41(7): 1164-1168.
[14] Muthukumaran S, Gopalakrishnan R. Structural, FTIR and photoluminescence studies of Cu doped ZnO nanopowders by co-precipitation method. *Opt. Mater*. 2012;34(11): 1946-1953.
[15] Ghomrani FZ, Aissat A, Arbouz H, Benkouider A, Al Concentration Effect on ZnO Based Thin Films: For Photovoltaic Applications. *Energy Procedia*. 2015;74: 491-498.
[16] Sreedhar A, Kwon JH, Yi J, Kim JS, Gwag JS. Enhanced photoluminescence properties of Cu-doped ZnO thin films deposited by simultaneous RF and DC magnetron sputtering. *Mater. Sci. Semicond. Process*. 2016;49: 8-14.
[17] Shukla RK, Srivastava A, Kumar N, Pandey A, Pandey M. Optical and Sensing Properties of Cu Doped ZnO Nanocrystalline Thin Films. *J. Nanotechnol*. 2015;2015: 1-10.
[18] Sounder J, Gowthaman P, Venkatachalam M, Saroja M, Parthasarathy G. ZNO Thin Film Prepared By Dip Coating Technique for Gas Sensing Application. *Int. J. Res. Appl. Sci. Eng. Technol*. 2017;5: 417-419.
[19] Azuma M, Ichimura M. Fabrication of ZnO thin films by the photochemical deposition method. *Mater. Res. Bull*. 2008;43: 3537-3542.
[20] Chichvarina O, Herng TS, Phuah KC, Xiao W, Bao N, Feng YP, Ding J. Stable zinc-blende ZnO thin films: formation and physical properties. *J. Mater. Sci*. 2015;50: 28-33.
[21] Khan M, Alam MS, Saha B, Ahmed SF. Synthesis and Characterization of Cadmium Sulfide (CdS) Thin Films by Cyclic Voltammetry Technique. *Materials Today: Proceedings*. 2021;47: 2351-2357.
[22] Abuelwafa AA, Denglawey AE, Dongol M, Nahass MME, Soga T. Influence of annealing temperature on structural and optical properties of nanocrystalline Platinum octa ethylporphyrin (PtOEP) thin films. *Opt. Mater*. 2015;49: 271-278.
[23] Ghosh PK, Maiti UN, Ahmed SF, Chattopadhyay KK. Highly conducting transparent nanocrystalline Cd1− xSnxS thin film synthesized by RF magnetron sputtering and studies on its optical, electrical and field emission properties. *Sol. Energy Mater. Sol. Cells*. 2006;90(16): 2616-2629.
[24] Mia MNH, Rana SM, Pervez MF, Rahman MR, Hossain MK, Mortuza AA, Basher MK, Hoq M. Preparation and spectroscopic analysis of zinc oxide nanorod thin films of different thicknesses. *Materials Science-Poland*. 2017;35(3): 501-510.
[25] Sumi M, Bella GR. Morphological, thermal and water absorption properties of polyvinyl alcohol/ZnO nanocomposites. *Int. J. Latest Trends Eng. Technol*. 2017: 226-232.
[26] Khan ZR, Khan MS, Zulfequar M, Khan MS. Optical and Structural Properties of ZnO Thin Films Fabricated by Sol-Gel Method. *Mater. Sci. App*. 2011;2: 340-345.
[27] Fattah ZA. Synthesis and characterization of Nickel doped Zinc Oxide nanaparticles by sol-gel method. *Int. J. Eng. Sci. Res. Techno*l. 2016;5: 418-429.
[28] Gayen RN, Sarkar K, Hussain S, Bhar R, Pal AK. ZnO films prepared by modified sol-gel technique. *Ind. J. Pure Appl. Phys*. 2011;49(7): 470-477.
[29] Mote VD, Huse VR, Dole BN. Synthesis and Characterization of Cr Doped ZnO Nanocrystals. *World J. Condens Matter Phys*. 2012;2(4): 208-211.
[30] Hao YM, Lou SY, Zhou SM, Yuan RJ, Zhu GY, LiN. Structural, optical, and magnetic studies of manganese-doped zinc oxide hierarchical microspheres by self-assembly of nanoparticles. *Nanoscale Res. Lett*. 2012;7: 1-13.
[31] Kayani ZN, Iqbal M, Riaz S, Zia R, Naseem S. Fabrication and properties of zinc oxide thin film prepared by sol–gel dip coating method. *Mater. Sci. Pol*. 2015;33(3): 515-520.

[32] Daranfed W, Guermat N, Bouchama I, Mirouh K, Dilmi S, Saeed MA. Effect of the Deposition Times on the Properties of ZnO Thin Films Deposited by Ultrasonic Spray Pyrolysis for Optoelectronic Applications. *J. Nano Electron. Phys*. 2019;11: 06001-06005.
[33] Ghosh PK, Maiti UN, Ahmed SF, Chattopadhyay KK. Photoluminescence and field emission properties of ZnS:Mn nanoparticles synthesized by rf-magnetron sputtering technique. *Opt. Mater*. 2007;29(12): 1584-1590.
[34] Caglar M, Yakuphanoglu F. Structural and optical properties of copper doped ZnO films derived by sol-gel. *Appl. Surf. Sci*. 2012;258(7): 3039-3044.
[35] Alam MS, Khan M, Ahmed SF. Nanostructure wrinkle thin films on flexible substrate: Tunable optical properties. To be published in *Materials Today: Proceedings*. [Preprint] 2021. Available from: doi.org/10.1016/j.matpr.2021.07.101.
[36] Jannane T, Manoua M, Liba A, Fazouan N, Hichou AE, Almaggoussi A, Outzourhit A, Chaik M. Sol-gel Aluminum-doped ZnO thin films: synthesis and characterization. *J. Mater. Environ. Sci*. 2017;8(1): 160-168.
[37] Rai RC. Analysis of the Urbach tails in absorption spectra of undoped ZnO thin films. *J. Appl. Phys*. 2013;113(15): 153508.
[38] Alam MS, Mukherjee N, Ahmed SF. Optical Properties of Diamond Like Carbon Nanocomposite Thin films. *AIP Conference Proceedings.* 2018;1953(1): 090018.
[39] Islam MA, Hossain MS, Aliyu MM, Chelvanathan P, Huda Q, Karim MR, Sopian K, Amin N. Comparison of Structural and Optical Properties of CdS Thin Films Grown by CSVT, CBD and Sputtering Techniques. *Energy Procedia*. 2013;33: 203-213.
[40] Bedia A, Bedia FZ, Aillerie M, Maloufi N, Benyoucef B. Influence of the thickness on optical properties of sprayed ZnO hole-blocking layers dedicated to inverted organic solar cells. *Energy Procedia*. 2014;50: 603-609.
[41] Alam MS, Ghosh CK, Mukherjee N, Ahmed SF. Nanostructure evolution and optical properties of silver doped diamond like carbon thin film on soft polymer. *Adv. Sci. Lett*. 2018;24(8): 5731-5736.
[42] Bedia A, Bedia FZ, Aillerie M, Maloufi N, Benyoucef B. Morphological and Optical Properties of ZnO Thin Films Prepared by Spray Pyrolysis on Glass Substrates at Various Temperatures for Integration in Solar Cell. *Energy Procedia*. 2015;74: 529-538.

THE AUTHORS

Khan M.
e-mail: khanmohibul2@gmail.com
ORCID: 0000-0002-3323-7843

Ahmed S.F.
e-mail: fahmed.phys@aliah.ac.in
ORCID: 0000-0002-7872-0230